Journal of Organometallic Chemistry, 419 (1991) 233–243
Elsevier Sequoia S.A., Lausanne
JOM 22127

Spectroscopic and electrochemical properties of the isomeric bidiazine complexes $[(C_5Me_5)ClRh(bdz)]^+$ and $(C_5Me_5)Rh(bdz)$ and their relevance to the catalysis of the $2\ H^+ \rightarrow H_2$ reaction by 2,2′-bipyridine analogues

Monika Ladwig and Wolfgang Kaim *

Institut für Anorganische Chemie, Universität Stuttgart, Pfaffenwaldring 55, W-7000 Stuttgart 80 (Germany)

(Received March 4th, 1991)

Abstract

Electronic structures and ligand effects have been studied for the isomeric $Rh^{III/I}$ complexes $[(C_5Me_5)ClRh(bdz)](X)$ and $(C_5Me_5)Rh(bdz)$; $X^- = Cl^-$, PF_6^-; bdz = bidiazines (3,3′-bipyridazine, 2,2′-bipyrazine, 2,2′- and 4,4′-bipyrimidine). Comparative NMR and UV–Vis spectroscopic as well as cyclic voltammetric measurements in aprotic solvents have allowed definition of a frontier MO situation that has been correlated with the reactivity of the $[(C_5Me_5)ClRh(bpy)]^+$ system as a catalyst for the evolution of hydrogen from water. Thus, while the potential for the two-electron reduction of the Rh^{III} halide precursor depends on the ligand basicity, the MO description shows that there is extremely strong π-back donation and orbital mixing between the d orbitals of the H^+-accepting $(C_5Me_5)Rh^I$ fragment and the acceptor level of the heterocyclic ligand.

Introduction

In two recent papers Kölle, Grätzel, and coworkers have reported on the mechanism of action of a homogeneous rhodium based system $[(C_5Me_5)ClRh(bpy)]^+$, bpy = 2,2′-bipyridine, which can catalyze the two-electron reduction of $2H^+$ to H_2 [1,2]. The catalytic cycle involves a two-electron reductive elimination of a ligand L (eq. 1), a rapid oxidative addition of the first H^+ to form a monohydride (eq. 2), and the protonation of this hydride to yield dihydrogen and re-coordination of the initially eliminated ligand L (eq. 3) [1,2].

$$L\text{–}[Rh^{III}]^+ + 2\,e^- \rightarrow [Rh^I] + L^- \quad (1)$$

$$[Rh^I] + H^+ \rightarrow H\text{–}[Rh^{III}]^+ \quad (2)$$

$$H\text{–}[Rh^{III}]^+ + H^+ + L^- \rightarrow L\text{–}[Rh^{III}]^+ + H_2 \quad (3)$$

(L^- e.g. Cl^-; [Rh] = $(C_5Me_5)Rh(\alpha\text{-diimine})$).

Other groups have tried to make use of this behaviour in terms of electrode coating [3] and coenzyme conversion [4]. In order to gain further understanding of

0022-328X/91/$03.50

the role of the electron-accepting α-diimine ligand during the reaction cycle and to evaluate possibilities for modification, we have prepared the analogous cationic complexes $[(C_5Me_5)ClRh(bdz)]^+$ as chloride or hexafluorophosphate salts with all four isomeric bidiazine chelate ligands shown below [5].

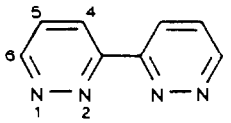

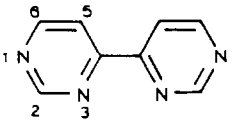

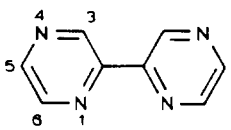

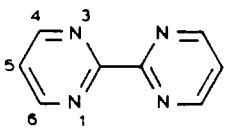

The four "diaza-2,2′-bipyridines" shown above are quite different in their ligand characteristics: Their basicities pK_{BH^+}, reduction potentials E_{red}, and electron distributions in the reduced state, as exemplified by the MO coefficients c_N^2 at the coordinating nitrogen centers, do not vary in a regular fashion (Fig. 1) [5,6].

It would be useful if these characteristics could be correlated with specific physical properties of interest in pertinent metal complexes. Previous systematic studies on Cr^0 [5], Mo^0 [5,7,8], W^0 [5], Ru^{II} [6], Re^I [9], Pt^{II} [10] and Cu^I [10] complexes have yielded optical, electrochemical, EPR and reactivity data which could be interpreted in terms of calculated or experimental α-diimine ligand properties.

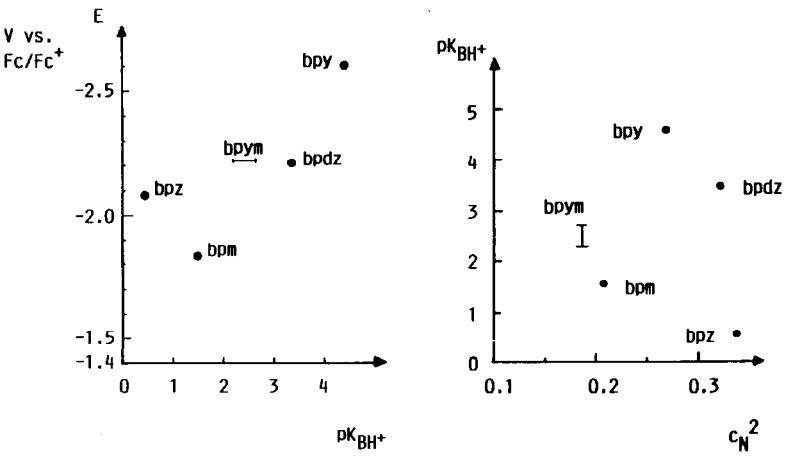

Fig. 1. Properties of 2,2′-bipyridine and the bidiazine ligands. Basicities pK_{BH^+} versus reduction potentials E (left) and versus the sum of squared LUMO (π_1^*) coefficients c_N^2 at the metal-coordinating centers (right).

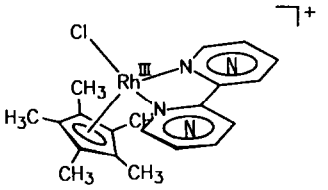

Fig. 2.

We now describe the synthesis and the NMR and UV–Vis spectroscopic characterization of all four rhodium(III) complexes (Fig. 2), and compare their cyclic voltammetric behaviour with that of the bpy analogue.

The optical spectra, some ^{1}H- and ^{13}C-NMR data, and the cyclic voltammetric response of the chemically or electrochemically generated rhodium(I) complexes $(C_5Me_5)Rh(bdz)$ (Fig. 3) as potentially proton-accepting intermediates [1,2] are also reported, and interpreted in terms of a frontier molecular orbital scheme.

Results and discussion

Synthesis and NMR spectroscopy

All four complexes (Fig. 2) were synthesized from $(C_5Me_5)_2(\mu\text{-}Cl)_2Cl_2Rh_2$ and the appropriate diimine ligand. The ^{1}H-NMR data are readily interpreted because of typical coupling patterns for the heteroaromatic protons, and are in good agreement with previous data for chelated bdz ligands [5–10]. The signals from the bdz ring protons are shifted to different extents from those for the free ligands; in particular, protons in *para* positions to (coordinated) nitrogen atoms are shifted most strongly downfield in the Rh^{III} cations. On the other hand, the protons of the heterocyclic groups in the Rh^{I} complexes, as obtained by potassium reduction of Rh^{III} precursors in THF, are distinguished by high-field shifts, especially in aromatic solvents such as C_6D_6. In particular, the 5,5′-position of the bpym ligand is affected by π-donor induced NMR shifts because the MO coefficient c^2 in the lowest unoccupied molecular orbital (LUMO, π_1^*) is very large at that position [11,12]. Thus, the neutral complex $(C_5Me_5)Rh(bpym)$ exhibits not only a relatively low $\delta(H^{5,5'})$ value of 6.03 ppm but also a very small and even more noteworthy ^{13}C chemical shift of only 112.4 ppm for the $C^{5,5'}$ centers [13]. The free bpym ligand has the corresponding signal at δ 120.6 ppm in that solvent. Similar effects are observed for the nuclei $H^{4,4'}$ and $C^{4,4'}$ in the position *para* to the coordination center in the complex $(C_5Me_5)Rh(bpdz)$ (cf. Experimental section). These results in themselves

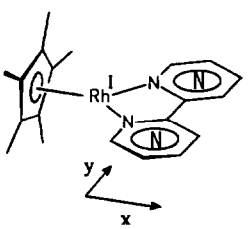

Fig. 3.

indicate a sizable amount of back-donation from the $(C_5Me_5)Rh^I$ fragment to the heterocyclic ligand.

Electrochemistry

Cyclic voltammetry of the complexes (Fig. 2) was performed at a standard scan rate of 100 mV/s in acetonitrile/0.1 *M* tetrabutylammonium hexafluorophosphate. In some experiments, the scan rate was varied in order to relate the observed behaviour of the new complexes with previously reported data [2].

Initially the oxidation of the cationic Rh^{III} complexes (as hexafluorophosphates) occurs in a highly irreversible fashion at about +1.5 V vs. Fc/Fc^+ for all isomers and the bpy complex. The small variation of ±0.1 V suggests an oxidation of metal-bound halide [14] or pentamethylcyclopentadienide ligand rather than an oxidation of Rh^{III}.

Reduction of the Rh^{III} complexes (Fig. 2) occurs at cathodic peak potentials between −1.0 and −1.4 V vs Fc/Fc^+ (Fig. 4, Table 1). As has been discussed in

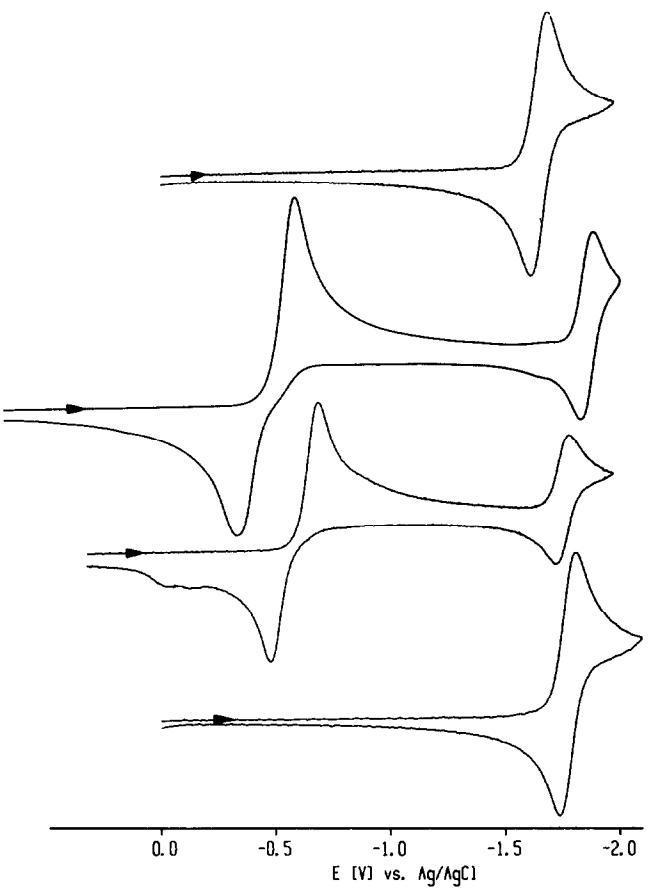

Fig. 4. Cyclic voltammograms (100 mV/s) of ligands and complexes in acetonitrile/0.1 *M* Bu_4NPF_6, from top to bottom: bpz, $[(C_5Me_5)ClRh(bpz)](PF_6)$, $[(C_5Me_5)ClRh(bpym)](Cl)$, bpym. Note the two-electron reduction of Rh^{III} cations and the one-electron reduction of the Rh^I complexes formed (Fc/Fc^+ +0.5 V vs. Ag/AgCl).

Table 1

Electrochemical data for the reduction of ligands, Rh^{III} and Rh^{I} complexes [a]

ligand	$[(C_5Me_5)ClRh(bdz)]^+$			$(C_5Me_5)Rh(bdz)$	bdz			
	E_{pc}	E_{pa}	$E_{pa} - E_{pc}$	$E_{red1}(\Delta E_{1/2})$ [b]: i_{pa}/i_{pc}	$E_{red1}(\Delta E_{1/2})$ [b,c]	ΔE_{red1} [d]	pK_{BH^+}	c_N^2 [g]
bpdz	−1.09	−0.80	0.29 [e]	−2.43(70):0.70	−2.24(70)	−0.19	3.37	0.326
bpm	−1.01	−0.83 [f]	0.18	−2.02(60):0.84	−1.86(90)	−0.14	1.5	0.208
bpz	−1.01	−0.73	0.28	−2.28(50):0.95	−2.12(60)	−0.16	0.45	0.340
bpym	−1.19	−1.01	0.18	−2.26(60):0.87	−2.24(70)	−0.02	≈ 2.5	0.190
bpy	−1.36	−1.06 [f]	0.30	−2.61(80):0.89	−2.57(100)	−0.04	4.4	0.278

[a] From cyclic voltammetry at 100 mV/s in CH_3CN/0.1 *M* tetrabutylammonium hexafluorophosphate. Potentials in V vs. Fc/Fc^+. [b] Peak potential difference in mV. [c] Peak current ratios $i_{pa}/i_{pc} > 0.7$. [d] Difference between reduction potentials of the Rh^I complex and of the free ligand. [e] 0.23 V at 20 mV/s, 0.30 V at 200 mV/s, 0.35 V at 500 mV/s, 0.38 V at 1000 mV/s, 0.42 V at 2000 mV/s. [f] Small anodic peak at about −0.5 V ($Rh^{II} \rightarrow Rh^I$). [g] Sum of calculated Hückel LUMO coefficients for both chelate coordination centers (ref. 5a).

detail for the bpy complex [2], this process is a typical two electron reductive elimination $d^6 \rightarrow d^8$ with undistorted yet distinctly separated peak waves. If the reduction occurs predominantly at the metal center, leading from Rh^{III} to Rh^{I}, the cathodic peak potentials should [6] correlate with the ligand basicities pK_{BH^+} which follow the order [5,6]: bpz < bpm < bpym < bpdz < bpy (Fig. 1).

This expectation is not completely fulfilled: while complexes of the weakest bases bpz and bpm do exhibit the least negative cathodic peak potentials and the bpy system is by far the most difficult to reduce, the bpdz complex is more easily reduced than the bpym analogue. One possible explanation involves mixing of metal d and low-lying unoccupied ligand π orbitals in the generated Rh^{I} complex, an effect which should shift E_{pc} of bpdz and bpz to more positive values because of their large MO coefficients at the metal-binding diimine centers, the metal–ligand interface [6].

The reduction of the Rh^{III} complexes (Fig. 2) is electrochemically irreversible, with peak potential differences $E_{pa} - E_{pc}$ exceeding 100 mV under the conditions of measurement (Table 1). According to previous studies of bpy systems, the mechanism involves a very rapid ECE process with facile loss of rhodium-bound halide ion in the course of the total two-electron reduction [1,2]. The thermally stable, though highly reactive, products of that process are the potentially H^+-uptaking neutral Rh^{I} species $(C_5Me_5)Rh(diimine)$ (Fig. 3). Depending on the diimine ligand and the scan rate, their oxidation can occur in a reverse fashion as a rapid two-electron process at still negative potentials with halide addition or, especially for bpy and bpym complexes, in two one-electron steps involving final oxidation of significant amounts of a Rh^{II} species [2] at about -0.5 V vs. Fc/Fc^+. Complexes with better reducible ligands such as bpm and bpz did not exhibit the latter signal under standard conditions, indicating the occurrence of a fairly rapid conversion $Rh^{II} \rightarrow Rh^{I}$. The appearance of the (assumed [1,2]) Rh^{II} signal as well as the difference between peak potentials of the two-electron process are dependent on the cyclovoltammetric scan rate; $E_{pa} - E_{pc}$ for complexes (Fig. 2) increases with the scan rate (Table 1), as reported previously for the bpy analogue [2].

The peak potential differences $E_{pa} - E_{pc}$ also illustrate the ligand response to the different oxidation states Rh^{III} and Rh^{I}. The observed large values for the bpdz and bpz isomers and the smaller numbers for the bpym and bpm complexes show a correlation with the calculated orbital coefficients ($c_N{}^2$, Fig. 1) at the coordinating nitrogen centers in the π_1^* orbital of the diimine ligand. An similar relationship is displayed by experimental ^{14}N and metal isotope EPR coupling constants in complexes of corresponding anion radical ligands [11,12].

A ready interpretation of this correlation between peak potential differences and the possible amount of π-back donation from the metal is that the Rh^{I} complexes are particularly stabilized by electron delocalization to the heterocyclic π acceptor ligand. An assessment of the relative degree of π back donation [15] can be made by comparing the potential for reversible *one-electron reduction* of the Rh^{I} product complexes with that for the free diimine ligands (cf. Fig. 4). These single electron waves invariably show half the peak current of the $Rh^{III/I}$ two electron signals (Fig. 4).

Normally, the coordination of a σ-electrophilic metal center to a reducible ligand facilitates its reduction by increasing the electronegativity of the metal coordinated donor center [16]. In some instances, however, the reverse flow of electron-density

via π-back donation can more than compensate for this effect, so that the complex is more difficult to reduce than the free π-acceptor ligand [15]. Such a situation is favoured by good metal/ligand π overlap and by a pronounced electron deficiency of the ligand acceptor or by a π electron excess on the metal donor. Whereas the former situation was recognized in complexes of carbonylmetal (Cr, Mn) fragments with extremely good π-accepting TCNE or TCNQ ligands [15], the latter alternative is obviously responsible for the effects observed (Fig. 4, Table 1) in case of complexes between the moderately π-accepting diimines and the very electron rich $(C_5Me_5)Rh$ group. Not unexpectedly, the (negative) difference $\Delta E_{red1} = E_{red1}$(Rh complex) – E_{red1}(ligand) (cf. Table 1) between the reduction potentials of the free diimine ligand and that of the corresponding complex $(C_5Me_5)Rh$(diimine) is most pronounced in case of the bipyrazine ligand, which is a poor base (weak σ-bonding) but an efficient π-acceptor (strong π back donation). The bpy and bpym ligands are better bases and weaker π-acceptors so that the two effects towards the $(C_5Me_5)Rh$ fragment are about equal and similar reduction potentials are consequently observed for the complex and the free ligand.

Electron addition to the complexes $(C_5Me_5)Rh$(diimine) is thus not confined to the diimine ligand alone (which has already received electron density via strong π back donation). Preliminary EPR investigations of the chemically generated (K/THF) anions $[(C_5Me_5)Rh(diimine)]^{-\cdot}$ did not produce signals detectable at room temperature—behaviour which would indicate rapid spin relaxation and thus suggest [15,16] significant metal participation in the singly occupied MO. In contrast, the less π-donating (diene)Rh^+ cations for which α-diimine complexes were reported [17–19] bind to reduced diimines with clear localization of the unpaired electron on the diimine ligand [18,19].

UV–Vis absorption spectroscopy

All Rh^{III} complexes (Fig. 2) show a band system between 300 and about 450 nm in the UV–Vis spectra (Fig. 5) with at least two visible maxima or shoulders. Interpretation of these bands and their energy variations is based on the results of electrochemical oxidation and reduction. We assume that these absorptions are caused by (chloride- or pentamethylcyclopentadienide-)ligand-to-metal charge transfer (very broad band at 360 nm) and by more distinct metal-to-diimine charge transfer transitions at typically (5–10) variable, generally somewhat higher, energies (Table 2).

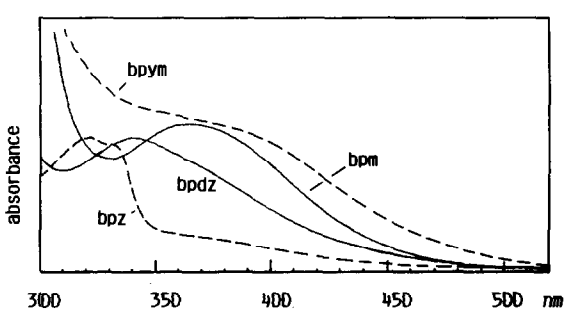

Fig. 5. Absorption spectra of Rh^{III} complexes $[(C_5Me_5)ClRh(bdz)]^+$ in dichloromethane solution. Absorbance scale different for each spectrum.

Table 2

UV–Vis absorption maxima λ_{max} (nm) for Rh^{III} and Rh^{I} complexes, in dichloromethane and THF, respectively

ligand	$[(C_5Me_5)ClRh(bdz)]^+$		$(C_5Me_5)Rh(bdz)$
	$Cl \rightarrow Rh^{III}$ CT	$Rh^{III} \rightarrow$ bdz CT	$Rh^{I} \rightarrow$ bdz CT
bpdz	360(sh)	341	531 [a]
bpm	375(sh)	364	535 [b]
bpz	360(sh)	330, 323	544 [c]
bpym	364(sh)	312(sh)	527 [d]
bpy	351(sh)	330 317	512 [c]

[a] Low intensity bands at 630(sh), 690(sh), 755, 850 nm. [b] Low intensity shoulders. [c] Ref. 2. [d] Low intensity bands at 660(sh), 775, 867, 988(sh) nm.

Metal-to-diimine charge transfer transitions should occur at much lower energies in the complexes (Fig. 3) of the Rh^{I} fragment. Intense (lg $\epsilon > 4$ [2]) such bands are, indeed, observed in a remarkably narrow spectral range of about $\lambda_{max} = 520$ nm for all the complexes $(C_5Me_5)Rh(diimine)$ (Fig. 6, Table 2). This unexpectedly [5–10] small variation is attributable to the molecular orbital situation shown in the qualitative MO diagram (Fig. 7) in which the energies of the π_1^* orbital and the symmetry-related π-donor orbital ($4d_{xz}$, cf. Fig. 3) are similar [15]. Stronger metal/ligand interaction due to larger c_N^2 values (Fig. 1), as in the bpz and bpdz complexes, thus results in slightly hypsochromically shifted transitions.

In contrast to complexes of organometallic fragments with $3d$ metals, such as chromium or manganese [15], which have π-type transitions between ligand/metal mixed orbitals in the near-infrared region (> 750 nm), the low-valent rhodium complexes (Fig. 3) have a main charge transfer band of relatively high energy.

Since the π-type interacting d_{xz} orbital is among the most stabilized in a pseudo-planar d^8 configuration, there are still three filled d orbitals of higher energy from which transitions to unoccupied MOs can occur at rather low energies (7). It is possible that the less intense bands or shoulders observed between 600 and 1000 nm

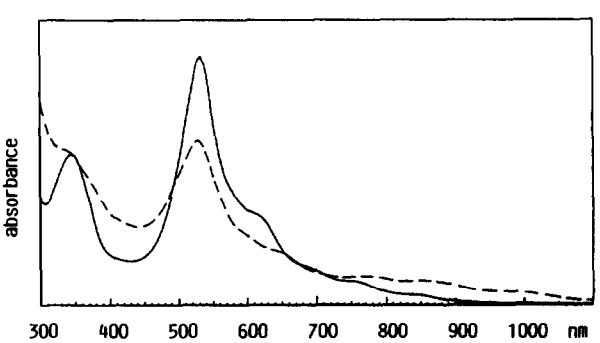

Fig. 6. Absorption spectra of Rh^{I} complexes $(C_5Me_5)Rh(bpdz)$ (———) and $(C_5Me_5)Rh(bpym)$ (- - - - -) in THF solution. Absorbance scale different for each spectrum.

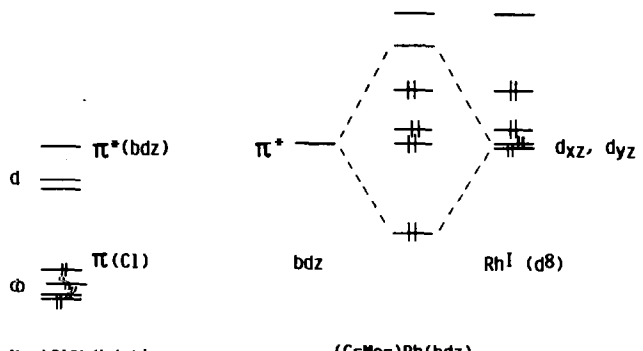

Fig. 7.

(Fig. 6) can be attributed to such symmetry- and overlap-disfavoured transitions; an alternative explanation would have to rely on parallels to the structured ($\Delta\tilde{\nu} \approx 1400$ cm^{-1}) low-intensity bands of singly reduced heterocyclic α-diimines [20,21] or quinones [22]. More intense metal-to-ligand charge transfer bands resulting from transitions to the second or third lowest unoccupied MOs $\pi^*_{2,3}$ of the heterocycles [5,23,24] are observed only at relatively high energies (< 370 nm, Fig. 6).

Conclusion

The present study, involving systematic ligand variation, has contributed to the understanding of the nature of a metal complex that catalyzes the two-electron reduction of H^+ to H_2 [1–4]. Spectroscopic and electrochemical data allowed both the characterization of the H^+-binding $(C_5Me_5)Rh$ complex fragment as very efficiently π-electron donating and the recognition of the potential "electron buffer" role of the π-electron accepting diimine ligand. While the bidiazine ligands may not be as useful as 2,2′-bipyridines in complexes for actual catalysis because of the presence of additional basic nitrogen sites and because of less negatively shifted threshold potentials (Table 1), the analysis of bonding in isomers depicted in Fig. 2 and 3 helps to clarify electronic structures and provides clues for further ligand modification.

Experimental

Electronic absorption spectra were recorded on a Bruins Instruments Omega 10 spectrometer (for Rh^I compounds in sealed cuvettes). ^{1}H- and ^{13}C-NMR spectra were recorded on a Bruker AC-250 instrument. Cyclic voltammetry was performed with a PAR 273 potentiostat and a PAR 175 function generator; the three-electrode configuration consisted of a glassy carbon working electrode, a Pt wire counter electrode and a saturated Ag/AgCl electrode as reference. The ferrocene/ferricinium couple was used as internal standard (ca. +0.50 V vs. Ag/AgCl). A 0.1 *M* solution of tetrabutylammonium hexafluorophosphate in dry acetonitrile served as electrolyte. Scan rates were varied between 20 and 2000 mV/s.

All reactions were carried out under argon. Dried solvents were freshly distilled immediately before use. Starting materials were used as supplied commercially (bpym, bpz, bpy, rhodium chloride complexes), or were synthesized as described previously [5].

General procedure for synthesis of the compounds $[(C_5Me_5)ClRh(bdz)]^+ X^-$

To a suspension of 0.2 g (0.32 mmol) of di-μ-chlorodichlorobis(pentamethylcyclopentadienyl)dirhodium(III) in 10 ml of methanol were added 123 mg (0.78 mmol) of the bidiazine ligand. After 3 h stirring the yellow solution had become clear, except in the case of the bpm system for which heating to reflux in ethanol for 8 h was needed. Complexes with chloride as external anion were obtained by reducing the volume to 2 ml and additing ether. Hexafluorophosphates were precipitated from the reaction mixture by adding 254 mg (1.56 mmol) of ammonium hexafluorophosphate.

bpdz isomer (as the chloride): Orange complex, yield 80%. ^{1}H-NMR (CD_3CN): δ 1.71 (s, 15H, C_5Me_5); 8.17 (dd, 2H, $H^{5,5'}$); 9.03 (d, 2H, $H^{6,6'}$); 9.47 ppm (d, 2H, $H^{4,4'}$); $J(H^4,H^5)$ 8.6, $J(H^5,H^6)$ 5.0 Hz. Found: C, 43.78; H, 4.57; N, 11.67. $C_{18}H_{21}Cl_2N_4Rh$ (467.20) calc.: C, 46.28; H, 4.53; N, 11.99%. As the hexafluorophosphate: Orange-yellow complex, yield 80%. Found: C, 36.58; H, 3.72; N, 9.79. $C_{18}H_{21}ClF_6N_4PRh$ (576.71) calc.: C, 37.49; H, 3.67; N, 9.72%.

bpm isomer (as the hexafluorophosphate): Yellow complex, yield 62%. ^{1}H-NMR (CD_3CN): δ 1.74 (s, 15H, C_5Me_5); 8.46 (dd, 2H, $H^{5,5'}$); 9.28 (d, 2H, $H^{6,6'}$); 9.54 ppm (d, 2H, $H^{2,2'}$); $J(H^2,H^5)$ 1.2, $J(H^5,H^6)$ 5.2 Hz. Found: C, 36.45; H, 3.84; N, 9.58%. $C_{18}H_{21}ClF_6N_4PRh$ (576.71) calc.: C, 37.49; H, 3.67; N, 9.72%.

bpz isomer (as the hexafluorophosphate): Yellowish complex, yield 74%. ^{1}H-NMR (CD_3CN): δ 1.70 (s, 15H, C_5Me_5); 8.90 (d, 2H, $H^{5,5'}$); 9.03 (d, 2H, $H^{6,6'}$); 9.70 ppm (s, 2H, $H^{3,3'}$); $J(H^5,H^6)$ 3.0 Hz. Found: C, 37.29; H, 3.69; N, 9.77. $C_{18}H_{21}ClF_6N_4PRh$ (576.71) calc.: C, 37.49; H, 3.67; N, 9.72%.

bpym isomer (as the chloride): Yellow complex, yield 88%. ^{1}H-NMR (CD_3CN): δ 1.73 (s, 15H, C_5Me_5); 7.97 (dd, 2H, $H^{5,5'}$); 9.21 (dd, 2H, $H^{6,6'}$); 9.27 ppm (dd, 2H, $H^{4,4'}$); $J(H^4,H^5)$ 4.85, $J(H^5,H^6)$ 5.8, $J(H_4,H_6)$ 2.0 Hz. Found: C, 44.56; H, 4.67; N, 11.59. $C_{18}H_{21}Cl_2N_4Rh$ (467.20) calc.: C, 46.28; H, 4.53; N, 11.99%.

bpy complex (as the hexafluorophosphate): Yellow complex, yield 84%. ^{1}H-NMR (CD_3CN): δ 1.65 (s, 15H, C_5Me_5); 7.81 (dt, 2H, $H^{5,5'}$); 8.24 (dt, 2H, $H^{4,4'}$); 8.37 (d, 2H, $H^{3,3'}$); 8.89 ppm (d, 2H, $H^{6,6'}$); $J(H^3,H^4)$ 8.0, $J(H^4,H^5)$ 8.0, $J(H^5,H^6)$ 5.5 Hz. Found: C, 40.26; H, 4.18; N, 4.98; Cl, 6.13; P, 5.30. $C_{20}H_{23}ClF_6N_2PRh$ (574.74) calc.: C, 41.80; H, 4.03; N, 4.87; Cl, 6.17; P, 5.39%.

General procedure for preparation of the compounds $(C_5Me_5)Rh(bdz)$

A suspension of 0.1 g (0.21 mmol) of $[(C_5Me_5)ClRh(bdz)]Cl$ and 33 mg (0.84 mmol) of potassium in 25 ml of THF was stirred for 4 h under reflux. The colour turned from yellow to deep purple. The mixture was cooled, the solids were filtered off, and the filtrate reduced to dryness. Column chromatography (1 cm × 50 cm) of a solution of the (very sensitive) product in pentane was performed at −40 °C on silica gel 60 silanised with diethylether/THF (3 : 1 v/v) as eluent. The product was isolated from the purple zone (yields ca. 40%); in some cases the NMR spectra showed the presence of free ligand as impurity. The complexes were too sensitive for elemental analysis.

(C_5Me_5)Rh(bpym)

^{1}H-NMR (C_6D_6): δ 1.75 (s, 15H, C_5Me_5); 6.03 (dd, 2H, $H^{5,5'}$); 8.23 (dd, 2H, $H^{4,4'}$); 8.86 ppm (dd, 2H, $H^{6,6'}$); $J(H^5,H^6)$ 5.8, $J(H^4,H^5)$ 3.6, $J(H^4,H^6)$ 2.0 Hz. ^{13}C-NMR (C_6D_6): δ 9.7 (Me), 89.3 (C_5Me_5), 112.4 ($C^{5,5'}$), 145.9 ($C^{6,6'}$), 155.6 ($C^{4,4'}$), 148.0 ppm ($C^{2,2'}$).

(C_5Me_5)Rh(bpdz)

^{1}H-NMR (C_6D_6): δ 2.09 (s, 15H, C_5Me_5); 6.13 (dd, 2H, $H^{5,5'}$); 6.90 (dd, 2H, $H^{4,4'}$); 8.13 ppm (dd, 2H, $H^{6,6'}$); $J(H^4,H^5)$ 8.5, $J(H^5,H^6)$ 4.4, $J(H^4,H^6)$ 2.3 Hz. ^{13}C-NMR (C_6D_6): δ 9.6 (Me), 92.0 (C_5Me_5), 110.2 ($C^{5,5'}$), 125.6 ($C^{4,4'}$), 134.4 ($C^{3,3'}$), 146.7 ($C^{6,6'}$).

(C_5Me_5)Rh(bpz)

^{1}H-NMR (C_6D_6): δ 1.64 (s, 15 H, C_5Me_5); 7.68 (dd, 2H, $H^{5,5'}$); 8.57 (d, 2H, $H^{6,6'}$); 8.83 ppm (d, 2H, $H^{3,3'}$); $J(H^3,H^5)$ 1.2, $J(H^6,H^5)$ 4.3 Hz. ^{13}C-NMR (C_6D_6): δ 9.3 (Me), 90.4 (C_5Me_5), 134.2 ($C^{5,5'}$), 138.0 ($C^{2,2'}$), 143.6 ($C^{6,6'}$), 145.3 ppm ($C^{3,3'}$).

Acknowledgements

This work was supported by grants from Deutsche Forschungsgemeinschaft (SFB 270), Volkswagenstiftung and Fonds der Chemischen Industrie.

References

1 U. Kölle and M. Grätzel, Angew. Chem., 99 (1987) 572; Angew. Chem., Int. Ed. Engl., 26 (1987) 568.
2 U. Kölle, B.-S. Kang, P. Infelta, P. Compte and M. Grätzel, Chem. Ber., 122 (1989) 1869.
3 S. Cosnier, A. Deronzier and N. Vlachopoulos, J. Chem. Soc., Chem. Commun., (1989) 1259.
4 (a) R. Ruppert, S. Herrmann and E. Steckhan, J. Chem. Soc., Chem. Commun., (1988) 1150; (b) E. Steckhan, S. Herrmann, R. Ruppert, E. Dietz, M. Frede and E. Spika, Organometallics, 10 (1991) 1568.
5 (a) S. Ernst and W. Kaim, J. Am. Chem. Soc., 108 (1986) 3578; (b) E.C. Alyea, J. Malito, S.D. Ernst, W. Kaim and S.J. Kohlmann, Polyhedron, 8 (1989) 921.
6 S.D. Ernst and W. Kaim, Inorg. Chem., 28 (1989) 1520.
7 B. Olbrich-Deussner and W. Kaim, J. Organomet. Chem., 340 (1988) 71.
8 S. Ernst, S. Kohlmann and W. Kaim, J. Organomet. Chem., 354 (1988) 177.
9 W. Kaim, H.E.A. Kramer, C. Vogler and J. Rieker, J. Organomet. Chem., 367 (1989) 107.
10 C. Vogler, Ph.D. Thesis, University of Stuttgart, 1990.
11 W. Kaim, Inorg. Chem., 23 (1984) 3365.
12 W. Kaim and S. Ernst, J. Phys. Chem., 90 (1986) 5010.
13 C. Overton and J.A. Connor, Polyhedron, 1 (1982) 53.
14 W. Kaim and S. Kohlmann, Inorg. Chem., 29 (1990) 2909.
15 B. Olbrich-Deussner, R. Groß and W. Kaim, J. Organomet. Chem., 366 (1989) 155.
16 W. Kaim, Coord. Chem. Rev., 76 (1987) 187; cf. also W. Kaim, V. Kasack, H. Binder, E. Roth and J. Jordanov, Angew. Chem., Int. Ed. Engl., 27 (1988) 1174.
17 M.P. Garcia, J.L. Millan, M.A. Esteruelas and L.A. Oro, Polyhedron, 6 (1987) 1427.
18 W.A. Fordyce, K.H. Pool and G.A. Crosby, Inorg. Chem., 21 (1982) 1027.
19 S. Kohlmann, V. Kasack, E. Roth and W. Kaim, J. Chem. Soc., Faraday Trans. 1, 85 (1989) 4047.
20 E. König and S. Kremer, Chem. Phys. Lett., 5 (1970) 87.
21 P.S. Braterman, J.-I. Song, S. Kohlmann, C. Vogler and W. Kaim, J. Organomet. Chem., 411 (1991) 207.
22 A. Dei and L. Pardi, Inorg. Chim. Acta, 181 (1991) 3.
23 E.S. Dodsworth and A.B.P. Lever, Coord. Chem. Rev., 97 (1990) 271.
24 W. Matheis and W. Kaim, Inorg. Chim. Acta, 181 (1991) 15.